Electric polarization observed in single crystals of multiferroic Lu_{2}MnCoO_{6}

S. Chikara, J. Singleton, J. Bowlan, D. A. Yarotski, N. Lee, H. Y. Choi, Y. J. Choi, and V. S. Zapf

Electric polarization observed in single crystals of multiferroic Lu_2MnCoO_6

S. Chikara,[1] J. Singleton,[1] J. Bowlan,[2] D. A. Yarotski,[2] N. Lee,[3] H. Y. Choi,[3] Y. J. Choi,[3] and V. S. Zapf[1]

[1] *National High Magnetic Field Laboratory, Los Alamos National Laboratory, Los Alamos, NM 87545, USA*
[2] *Center for Integrated Nanotechnologies, Los Alamos National Laboratory, Los Alamos, NM 87545, USA*
[3] *Department of Physics and IPAP, Yonsei University, Seodaemun-gu, Seoul, 120-749, South Korea*

We report electric polarization and magnetization measurements in single crystals of double perovskite Lu_2MnCoO_6 using pulsed magnetic fields and optical second harmonic generation (SHG) in DC magnetic fields. We observe well-resolved magnetic field-induced changes in the electric polarization in single crystals and thereby resolve the question about whether multiferroic behavior is intrinsic to these materials or an extrinsic feature of polycrystals. We find electric polarization along the crystalline **b**-axis, that is suppressed by applying a magnetic fields along **c**-axis and advance a model for the origin of magnetoelectric coupling. We furthermore map the phase diagram using both capacitance and electric polarization to identify regions of ordering and regions of magnetoelectric hysteresis. This compound is a rare example of coupled hysteretic behavior in the magnetic and electric properties. The ferromagnetic-like magnetic hysteresis loop that couples to hysteretic electric polarization can be attributed not to ordinary ferromagnetic domains, but to the rich physics of magnetic frustration of Ising-like spins in the axial next-nearest neighbor interaction model.

I. INTRODUCTION

Multiferroics are materials that exhibit more than one primary ferroic order parameter in a single phase.[1–3] The most commonly studied combination is ferromagnetic and ferroelectric (FE) order, which can in turn give rise to magnetoelectric coupling.[4–6] Lu_2MnCoO_6 is a double perovskite material (also reported as Lu_2CoMnO_6 in the literature[7]) in which magnetic order breaks spatial inversion symmetry and thereby induces ferroelectricity. Usually in single-phase materials, magnetic order that induces electric polarization involves complex, often non-collinear structures that have little or no net magnetization. Unlike such materials, Lu_2MnCoO_6 is a rare example of a bulk multiferroic that exhibits strong, coupled ferromagnetic-like magnetization M and ferroelectric-like electric polarization P, both of which show hysteresis in response to changing magnetic field H and/or temperature T.[8]

Lu_2MnCoO_6 crystallizes in a $P2_1/n$ space group, in a double perovskite structure with a slight monoclinic distortion.[7,8] The Co^{4+} and Mn^{2+}ions alternate along the **c**-axis in distorted corner-sharing oxygen octahedra. This system orders antiferromagnetically at $T_N = 48$ K and below a second temperature, $T_H = 35$ K, there is the onset of the above-mentioned magnetic and electric-polarization hysteresis with applied magnetic field, plus strongly frequency-dependent magnetic and electric properties.[8,9] Elastic neutron-scattering measurements identify magnetic order with a net microscopic magnetization $M = 0$ at $H = 0$, despite the observed magnetic hysteresis loop that develops in applied H.[8] The magnetic ordering consists of **c**-axis chains of $Co(\uparrow)$- $Mn(\uparrow)$- $Co(\downarrow)$- $Mn(\downarrow)$ or $Mn(\uparrow)$- $Co(\uparrow)$- $Mn(\downarrow)$- $Co(\downarrow)$,[8,9] which are consistent with ab-initio calculations.[10] Magnetization measurements on single crystals demonstrate significant anisotropy in magnetic properties with hysteresis occuring only for H along the easy axis,[7] indicating Ising-like behavior. The orbital occupations of Co^{2+}

and Mn^{4+} suggest Co^{2+} as the likely source of most of the anisotropy.[11]

Muon-spin rotation (μ-SR), elastic neutron diffraction and bulk property measurements of Lu_2MnCoO_6 show consistency[9] with a variant of the axial next-nearest neighbor interaction (ANNNI) model.[12,13] In the ANNNI model, frustration between nearest and next-nearest neighbor Ising-like spins gives rise to a very rich phase diagram with hundreds of micro-phase transitions between states with different long-wavelength incommensurations, and ultimately an $\uparrow\uparrow\downarrow\downarrow$ ground state at $T = 0$ materializes for certain ratios of exchange interactions. Besides the rich spectrum of phases, there is a continuum of low-lying excitation states that can generate the hysteresis and dynamics observed in this system. In the ANNNI picture, the transition from reversible to hysteretic behavior would correspond to the freezing of spin-flip excitations in the $\uparrow\uparrow\downarrow\downarrow$ state. These frustrated magnetic interactions can give rise to magnetic hysteresis in a system that is not a simple ferromagnet with domains; such a system can have the necessary low symmetry to sustain electric polarization. The $\uparrow\uparrow\downarrow\downarrow$ ground state has also previously been observed in the compound Ca_3CoMnO_6, which produces an electric polarization along the **c**-axis due to symmetric exchange striction.[11,14,15] However, in Lu_2MnCoO_6, we will show that the electric polarization points along the **b**-axis. While coupled electric polarization and magnetization were observed in polycrystalline samples of Lu_2MnCoO_6 for both **H** $\parallel$ **c** and **H** $\perp$ c,[8] previous single-crystal studies were unable to detect electric polarization.[7] The single-crystal work did show a peak in the dielectric constant near $T = 35$ K for electric fields along the **b**-axis that is suppressed by magnetic fields applied along the **c**-axis. Here, we report both electric polarization and dielectric measurements as a function of magnetic field in single crystals of Lu_2MnCoO_6. This establishes that the multiferroic behavior is an intrinsic effect and not due to grain boundaries or other extrinsic effects of polycrys-
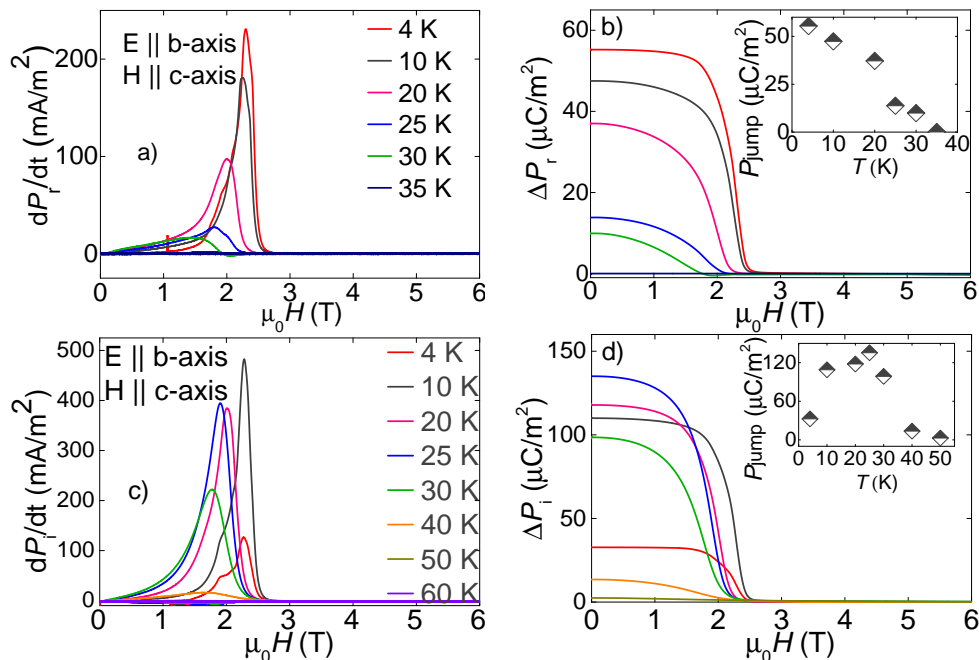
FIG. 1. The top two figures show the remanent electric polarization $\Delta P_r(H) = P_r(H) - P_r(0)$ measured in $E = 0$ in pulsed magnetic field H for different temperatures T. Sample was previously poled by cooling through T_N in an applied E and $H = 0$. (a) Shows the raw data dP_r/dt and (b) the integrated $\Delta P_r(H)$. The bottom two figures show the induced electric polarization $\Delta P_i(H)$ measured with E applied during the measurements in pulsed magnetic fields H for different temperatures T. Sample was previously cooled through T_N in $E = H = 0$. (c) shows the raw data $dP_i(H)/dt$ and (d) the integrated signal $\Delta P_i(H)$. The insets shows the magnitude of the magnetic field-induced jump P_{jump} between 0 and 6 T in $\Delta P_r(H)$ and $\Delta P_i(H)$ for different T. All data are for $\mathbf{H} \parallel \mathbf{c}$ and $\mathbf{E} \parallel \mathbf{b}$.

tals.[8]

II. EXPERIMENTAL DETAILS

The single crystals were grown using a flux technique.[7] Contacts for capacitance and electric polarization measurement were made by sputtering platinum and attaching leads with silver epoxy. Magnetic field pulses of 10 and 60 T with a sweep rate $\mu_0 dH/dt$ of up to 11.62 kT/sec for the upsweep of the pulse were applied using a capacitatively-driven resistive 65 T magnet.[16] The magnetoelectric current dP/dt, is generated as charges are drawn from ground to the sample contacts to screen the sample's surface charge as it changes with magnetic field.[8,17] The change in electric polarization $\Delta P = P(H) - P(H = 0)$ is obtained by numerically integrating dP/dt. The magnetoelectric current in response to the time-varying magnetic field was recorded with a Stanford Research 570 current-to-voltage converter at a data acquisition rate of 1 MHz. The resolution of these measurements increases with the square root of dH/dt and can exceed that of comparable superconducting-magnet measurements with $\mu_0 dH/dt \approx 0.01$ T/s by three orders of magnitude.[11,17,18] Data shown in the figures were taken with an electric field of 3.8×10^5 V/m (maximum electric field that can be used with ^{4}He) applied be-

fore or during the measurement. Different electric fields up to this maximum value were applied and a linear dependence of the electric polarization on electric field was observed, with a small offset attributable to stray electric fields due to schottky barriers at contacts and thermoelectric voltages.

Magnetization was measured using pulsed-field extraction magnetometry.[19,20] The sample was cooled by immersion in ^{3}He or ^{4}He and the temperature recorded approximately 1 s before the magnetic field pulse. The magnetic field is determined by integrating the voltage induced in a coil close to the field center, and calibrated by observing the de Haas-van Alphen oscillations of copper.[20]

Optical Second Harmonic Generation (SHG) was measured at $H = 0$. The measurement geometry is shown in Fig. 3. A 800 nm, 100 fs laser pulse is incident on the Lu_2MnCoO_6 crystal at approximately 45°. The 400 nm SHG signal is detected with a Photo Multiplier Tube using a lock-in amplifier. The 800 nm light is rejected by a 10 nm interference filter passing 400 nm, and a BG40 colored glass filter. The output polarization, $\mathbf{E}$ parallel to the plane of incidence (P-out) / $\mathbf{E}$ perpendicular to the plane of incidence (S-out) is selected with a Glan-Taylor polarizer. We measured the input polarization dependence of the S- and P- polarized components of the SHG signal from 5 to 200 K. The crystal was dry-polished to

a roughness 250 nm with diamond paper. The **b**-axis is normal to the sample surface, and the **a**- and **c**- axes are rotated 45° to the plane of incidence.

III. EXPERIMENTAL RESULTS AND DISCUSSION

The electric polarization was measured while sweeping the magnetic field in two different ways. First by poling (cooling through T_N in an electric field E at $H = 0$) and then setting the applied E to zero and measuring the change in polarization, $\Delta P_r(H)$. In the other set of measurements, the sample is first cooled through T_N with $E = H = 0$. Next, $E = 3.8 \times 10^5$ V/m is applied; the magnetic field is pulsed while the electric polarization change, $\Delta P_i(H)$ is recorded. These data measures field-induced capacitance changes, $C(H) - C(H = 0) = 1/E[P_i(H) - P_i(0)]$.

Figures 1 (a) and (b) show the remanent electric polarization as a function of magnetic field $\Delta P_r(H) = P_r(H) - P_r(0)$, and the raw $dP_r(H)/dt$ data from which it was derived. The data are shown for $\mathbf{E} \parallel \mathbf{b}$ and $\mathbf{H} \parallel \mathbf{c}$. All other combinations of $\mathbf{E}$ and $\mathbf{H}$ along the **a**, **b**, **c**-axes were also measured; however, no electric polarization was detected using these combinations. The observation of $\Delta P_r(H)$ only along $\mathbf{E} \parallel \mathbf{b}$ for $\mathbf{H} \parallel \mathbf{c}$ is consistent with the single-crystal dielectric measurements in applied magnetic field reported earlier.[7] These data at first sight seem inconsistent with the polycrystal result that finds $\Delta P_r(H)$ for both $\mathbf{H} \parallel \mathbf{P}$ and $\mathbf{H} \perp \mathbf{P}$. However, the latter result could be ascribed to magnetic dipole interactions between grains of the polycrystals.[8]

$\Delta P_r(H)$ measured in the single crystals of the current study is an order of magnitude larger than what was observed in polycrystalline samples, which is to be expected for a uniaxial electric polarization.[7,8] In Fig. 1 (a) and (b), there is an onset of remanent electric polarization $\Delta P_r(H)$ just below $T_H = 35$ K. Similarly, there is an onset of magnetic hysteresis at this temperature in the $M(H)$ data, also seen in previous poly- and single-crystal measurements.[8,21] $\Delta P_r(H)$ is suppressed in magnetic fields above ≈ 2 T, which corresponds to the coercive magnetic field in the $M(H)$ hysteresis loop for $\mathbf{H}\parallel\mathbf{c}$. This H and T dependence of ΔP_r is consistent with the previous polycrystalline results.[8]

On the other hand, Figures 1 (c) and (d) show the electric polarization $\Delta P_i(H)$ that is induced by a DC electric field that is applied during the magnetic field pulse. A non-zero change in P_i with H is observed for $T < T_N = 50$ K, rather than below $T_H = 35$ K as was seen for ΔP_r. The dielectric response $\Delta P_i(H)$ does show a peak near $T_H = 35$ K, however, which is consistent with the previous capacitance measurements of single- and polycrystal samples in quasistatic superconducting magnets.[7,8] The magnitude of our measured $\Delta P_i(H)$ is three times larger than our measured $\Delta P_r(H)$ at 4 K.

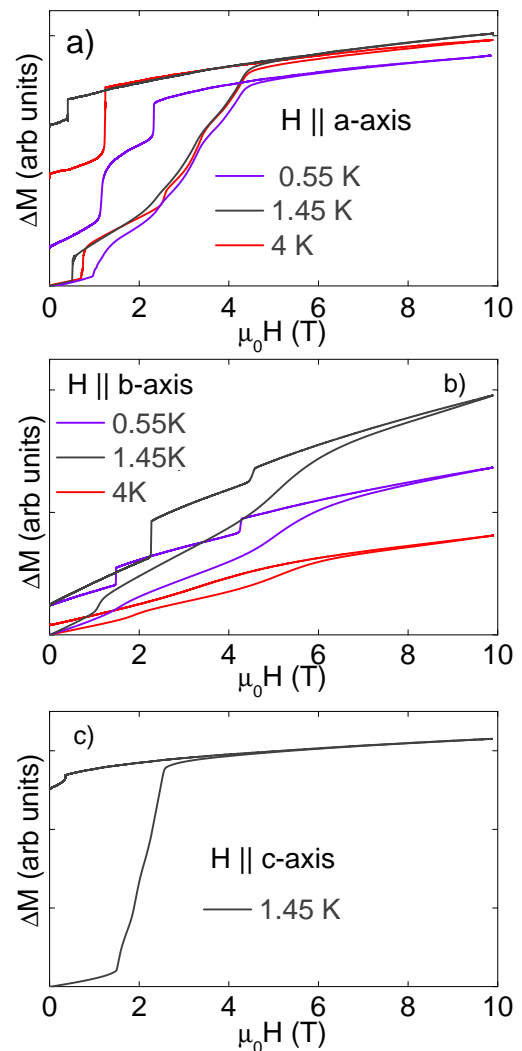We show the magnetization in pulsed magnetic fields

FIG. 2. Magnetization change $\Delta M = M(H) - M(H = 0)$ vs magnetic field H in pulsed magnetic fields for H along the a) a-axis, b) b-axis and c) c-axis. The pulsed data along different axes are not to scale - note the DC magnetization data show the c-axis magnetization to be significantly larger than along a or b.[7]

$\Delta M(H) = M(H) - M(H = 0)$ for $\mathbf{H}$ along the **a**, **b** and **c**-axes in Fig. 2. $\Delta M(H)$ for $\mathbf{H} \parallel \mathbf{c}$ is hysteretic in field and consistent with previous results in pulsed and DC fields for single- and polycrystals.[7,8] The coercive magnetic field is 2.0 T at 1.5 K. On the other hand, $\Delta M(H)$ for $\mathbf{H} \parallel \mathbf{a}$ and $\mathbf{H} \parallel \mathbf{b}$ differs from previous single crystal results in DC fields. $\Delta M(H)$ in pulsed fields shows hysteresis and step-like behavior while $M(H)$ in DC magnets is smooth, continuous, and non-hysteretic. Similar steps in the magnetization, electric polarization and magnetostriction were observed in Ca_3CoMnO_6 induced by certain ranges of magnetic field sweep rates between 75 and 1,500 T/s while smooth behavior was observed for both faster and slower sweep rates.[22] In Lu_2MnCoO_6 $P(H)$ is zero for the field orientations where steps are
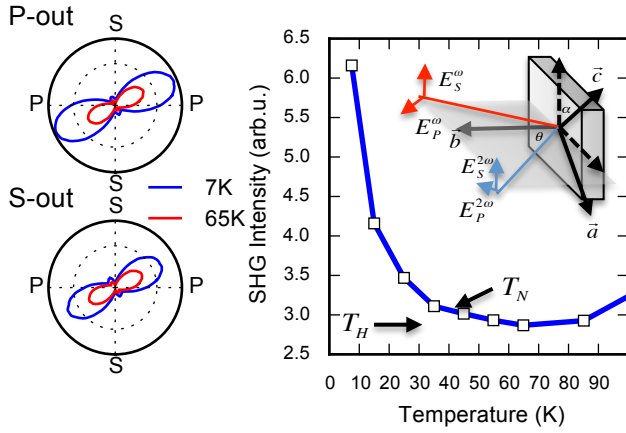
FIG. 3. The optical SHG measurements on Lu_2MnCoO_6 single crystal. The figure on the left shows the P-out and S-out polarization component. The change in the symmetry between 7 and 65 K is apparent. The right panel shows the SHG intensity as a function of temperature with rapid increase in intensity below 35 K. $E_S^{2\omega}$ and $E_P^{2\omega}$ are the S and P components of the second harmonic polarization respectively. The inset shows the measurement geometry.
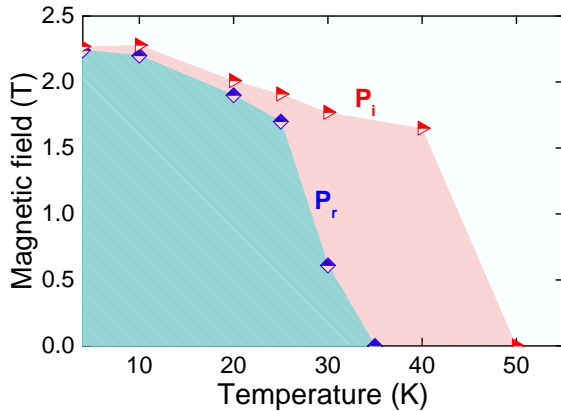

FIG. 4. The magnetic field vs temperature phase diagram showing the region where the remanent polarization ΔP_r and the induced polarization ΔP_i are non-zero. The region of nonzero ΔP_i corresponds to magnetic ordering in thermodynamic neutron diffraction measurements while ΔP_r corresponds to magnetic and electric hysteresis.

seen in pulsed-field $\Delta M(H)$ to 1700 T/s.[23] In similar systems like Ca_3CoMnO_6 and $Ca_3Co_2O_6$, many theories have been advanced for the origin of the metastable steps, most recently the presence of excited metastable states with high degeneracy due to frustration in Ising-like spins.[24]
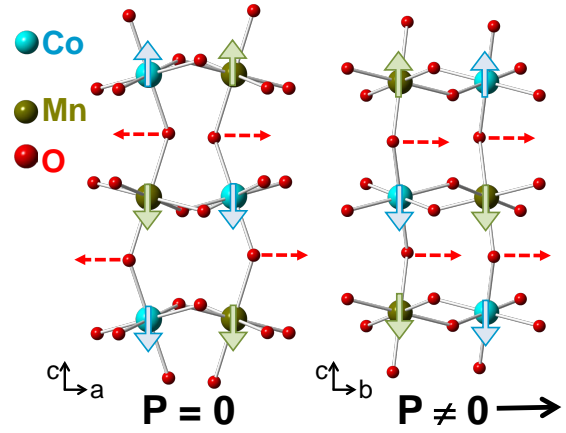
We measured the optical second harmonic genera-

FIG. 5. The projection of Lu_2CoMnO_6 structure in the (a) ac and (b) bc planes. The red arrows indicate the direction of oxygen displacement in response to the bond shortening or elongation due to the exchange between parallel or antiparallel spins on neighboring ions.

tion (SHG) in reflection from the single crystal of Lu_2MnCoO_6. The **b**-axis is normal to the sample surface, and the **a** and **c** axes are rotated 45 ° to the plane of incidence. A small SHG signal is observed at all temperatures up to 300 K. This signal most likely originates from the crystal surface where inversion symmetry is broken.[25,26] The SHG signal amplitude is essentially flat down to 40 K, and below 40 K the SHG signal begins to rise rapidly indicating that inversion symmetry has been broken. This pattern is consistent with the behavior of paraelectric / ferroelectric phase transitions in many other materials, [25] and is strong evidence that Lu_2MnCoO_6 is ferroelectric below the temperature, T_H = 35 K, where hysteretic polarization appears.

Figure 4 shows the (T, H) phase diagram of Lu_2MnCoO_6 from the $\Delta P(H)$ and $\Delta M(H)$ measurements performed in pulsed magnetic fields. The remanent electric polarization $\Delta P_i(H)$ is nonzero below T = 35 K, whereas the polarization induced by applied electric fields during the measurement $\Delta P_i(H)$ is nonzero below a higher temperature of 50 K. This implies that the capacitance shows an enhancement and a magnetic field dependence below the magnetic ordering temperature of 50 K. On the other hand, the hysteresis in the electric polarization, measured by $\Delta P_r(H)$, becomes finite below the temperature where hysteresis in T and H turns on in the magnetization at 35 K.[8,9]

Lu_2MnCoO_6 shows many similarities to Ca_3CoMnO_6 which also contains chains of alternating Mn^{4+} and Co^{2+} spins, although the oxygen cages have different symmetry.[8,27] In that compound the magnetic ground state is also ↑↑↓↓ along **c**-axis chains. The important difference is that in Ca_3CoMnO_6 $P(H)$ is observed along the **c**-axis, while in Lu_2MnCoO_6 $P(H)$ is seen for **P** ∥ **b** with **H** ∥ **c**. The two compounds have different crystal structures; Ca_3CoMnO_6 is not a double perovskite. In Lu_2MnCoO_6

we can understand the electric polarization along the **c**-axis due to the presence of oxygen bonds all canted along **b** direction.[10]

Figure 5 (a) and (b) shows the crystal structure of Lu_2MnCoO_6 in the bc and ac planes. If P results from an exchange-striction mechanism in the magnetically ordered phase, we can expect that the bonds between ferromagnetically-aligned spins contract while antiferromagnetically aligned spins repel. (Even if the opposite is the case i.e. [ferromagnetically-aligned spins repel while antiferromagnetically-aligned spins attract], the conclusion will be the same). When exchange striction distorts the bonds, the displacements of negatively-charged oxygens relative to positively-charged Mn and Co ions are indicated with arrows. It can be seen that along the b-axis, the net electric polarization change due to oxygen displacement in bonds subject to exchange striction on neighboring chains is non-zero while along all other axes, the oxygen displacements on neighboring chains cancel each other out. A net P along **b** was also predicted for isostructural Y_2MnCoO_6[10] in an $\uparrow\uparrow\downarrow\downarrow$ magnetic ground state scenario for similar reasons. The magnetic field-induced suppression of P occurs abruptly near the saturation magnetization where $\uparrow\uparrow\downarrow\downarrow$ state transitions to $\uparrow\uparrow\uparrow\uparrow$.

In conclusion, we demonstrate electric polarization in single crystals of Lu_2MnCoO_6 for the first time, by using a sensitive pulsed-magnetic-field and optical second-harmonic-generation techniques. We find that Lu_2MnCoO_6 is polar along the **b**-, and not along the **c**-axis. We show that a dielectric response emerges below the magnetic ordering temperature T_N while a hysteretic electric response occurs in the region of (T, H) phase space corresponding to hysteresis in the magnetization. We ascribe the origin of the field-induced electric polarization change to exchange striction coherently displacing oxygen ions along the **b**-axis. We also report additional metastable steps in the magnetization at finite magnetic field sweep rates up to 1700 T/s that do not occur at superconducting magnet sweep rates.

[1] N. A. Spaldin and M. Fiebig, Science , 391 (2005).

[2] D. I. Khomskii, J. Magn. Magn. Mater **306**, 1 (2006).

[3] D. Khomskii, Physics **2**, 20 (2009).

[4] W. Eerenstein, N. Mathur, and J. Scott, Nature , 759 (2006).

[5] S. Cheong and M. Mostovoy, Nature Materials **6**, 13 (2007).

[6] M. Bibes and A. Barthélémy, Nature Materials , 425 (2008).

[7] N. Lee, H. Y. Choi, Y. J. Jo, M. S. Seo, S. Y. Park, and Y. J. Choi, Appl. Phys. Letters **104**, 112907 (2014).

[8] S. Yáñez-Vilar, E. D. Mun, V. S. Zapf, B. G. Ueland, J. S. Gardner, J. D. Thompson, J. Singleton, M. Sánchez-Andújar, J. Mira, N. Biskup, M. A. Señarís-Rodríguez, and C. D. Batista, Phys. Rev. B **84**, 134427 (2011).

[9] V. S. Zapf, B. G. Ueland, M. Laver, M. Lonsky, M. Pohlit, J. Müller, T. Lancaster, J. S. Möller, S. J. Blundell, J. Singleton, J. Mira, S. Yañez-Vilar, and M. A. Señarís-Rodríguez, ArXiv e-prints (2014), arXiv:1409.5072 [cond-mat.mtrl-sci].

[10] C. Xin, Y. Sui, Y. Wang, Y. Wang, X. Wang, Z.-G. Liu, B. Li, and X. Liu, RSC Adv. , 43432 (2015).

[11] J. W. Kim, Y. Kamiya, E. D. Mun, M. Jaime, N. Harrison, J. D. Thompson, V. Kiryukhin, H. T. Yi, Y. S. Oh, S.-W. Cheong, C. D. Batista, and V. S. Zapf, Phys. Rev. B **89**, 060404 (2014).

[12] P. Bak, Rep. Prog. Phys. **45**, 587 (1982).

[13] W. Selke, Physics Reports **170**, 213 (1988).

[14] Y. J. Choi, H. T. Yi, S. Lee, Q. Huang, V. Kiryukhin, and S.-W. Cheong, Phys. Rev. Lett. **100**, 047601 (2008).

[15] Y. J. Jo, S. Lee, E. S. Choi, H. T. Yi, W. Ratcliff, Y. J. Choi, V. Kiryukhin, S. W. Cheong, and L. Balicas, Phys. Rev. B **79**, 012407 (2009).

[16] J. Singleton, C. Mielke, A. Migliori, G. S. Boebinger, and A. H. Lacerda, Physica B , 346 (2004).

[17] V. S. Zapf, M. Kenzelmann, F. Wolff-Fabris, F. Balakirev, and Y. Chen, Phys. Rev. B **82**, 060402(R) (2010).

[18] V. S. Zapf, P. Sengupta, C. D. Batista, F. Nasreen, F. Wolff-Fabris, and A. Paduan-Filho, Phys. Rev. B **83**, 140405 (2011).

[19] J. A. Detwiler, G. M. Schmiedeshoff, N. Harrison, A. H. Lacerda, J. C. Cooley, and J. L. Smith, Physical Review B **61**, 402 (2000).

[20] P. A. Goddard, J. Singleton, P. Sengupta, R. D. McDonald, T. Lancaster, S. J. Blundell, F. L. Pratt, S. Cox, N. Harrison, J. L. Manson, H. I. Southerland, and J. A. Schlueter, New Journal of Physics **10**, 083025 (2008).

[21] N. Lee, H. Y. Choi, Y. J. Jo, M. S. Seo, S. Y. Park, and Y. J. Choi, Applied Physics Letters **104**, 112907 (2014).

[22] J. W. Kim, E. D. Mun, A. Hansen, M. Jaime, N. Harrison, J. D. Thompson, H. T. Yi, Y. S. Oh, S.-W. Cheong, and V. S. Zapf, Unpublished.

[23] See Supplemental Material at [] for the magnetic field sweep rate vs magnetic field.

[24] Y. Kamiya and C. D. Batista, Phys. Rev. Lett. **108**, 097202 (2012).

[25] S. A. Denev, T. T. A. Lummen, E. Barnes, A. Kumar, and V. Gopalan, JACS , 1551 (2011).

[26] M. Fiebig, V. V. Pavlov, and R. V. Pisarev, J. Opt. Soc. Am. B , 96 (2005).

[27] S. Kaushik, S. Rayaprol, J. Saha, N. Mohapatra, V. Siruguri, P. Babu, and S. Patnaik, J. Appl. Phys. **108**, 084106 (2011).